

# Lawrence Berkeley National Laboratory

## Lawrence Berkeley National Laboratory

**Title**

Contribution of Eu 4f states to the magnetic anisotropy of EuO

**Permalink**

<https://escholarship.org/uc/item/6pb6s6mm>

**Author**

Arenholz, E.

**Publication Date**

2009-03-02

# Contribution of Eu $4f$ states to the magnetic anisotropy of EuO

E. Arenholz,<sup>1</sup> A. Schmehl,<sup>2</sup> D. G. Schlom,<sup>3</sup> and G. van der Laan<sup>4</sup>

<sup>1</sup>*Advanced Light Source, Lawrence Berkeley National Laboratory, Berkeley, CA 94720*

<sup>2</sup>*Institut für Physik, Universität Augsburg, Augsburg, Germany*

<sup>3</sup>*Department of Materials Science and Engineering,  
Cornell University, Ithaca, NY 14853-1501*

<sup>4</sup>*Diamond Light Source, Chilton, Didcot,  
Oxfordshire OX11 0DE, United Kingdom*

(Dated: September 8, 2008)

## Abstract

Anisotropic x-ray magnetic linear dichroism (AXMLD) provides a novel element-, site-, shell- and symmetry-selective technique to study the magnetic anisotropy induced by a crystalline electric field. The weak Eu<sup>2+</sup>  $M_{4,5}$  AXMLD observed in EuO(001) indicates that the Eu  $4f$  states are not rotationally invariant and hence contribute weakly to the magnetic anisotropy of EuO. The results are contrasted with those obtained for  $3d$  transition metal oxides.

PACS numbers: 78.70.Dm, 78.20.Bh, 75.30.Gw, 75.50.Dd

Magnetic anisotropy is a critical property to be tailored in the development of novel materials ranging from soft materials for magnetic cores used in power supplies and digital telecommunication equipment [1] to very hard materials for permanent magnet applications like motors and generators [2, 3]. For magnetic media used in information storage technology, the magnetic anisotropy has to be precisely tuned to allow for writing magnetic domains while avoiding loss of information in small external fields or at slightly elevated temperatures [4]. Due to its small size ( $10^{-5}$  to  $10^{-3}$  eV) [5], identifying the microscopic origin of the magnetic anisotropy in multi-element alloys and complex multilayered systems is non-trivial and it remains challenging to develop a detailed theoretical understanding of its origin.

Large anisotropic x-ray magnetic linear dichroism (AXMLD) at the  $L_{2,3}$  x-ray absorption (XA) edge has been reported from  $3d$  transition metal oxides [6–8]. It was shown that the angular dependence of the x-ray magnetic linear dichroism (XMLD) does not only depend on the orientations of the linear x-ray polarization,  $\mathbf{E}$ , and the sample magnetization,  $\mathbf{H}$ , but also on the relative orientation of these two vectors with respect to the crystallographic axes. In cubic symmetry, the AXMLD can be written as a linear combination of two different spectra, the so-called fundamental spectra. To obtain an anisotropy requires breaking of the spherical symmetry by a crystalline electric field (CEF), whereas the presence of spin-orbit interaction is not essential. The latter suggests that the AXMLD is not directly related to the magnetocrystalline anisotropy energy (MAE), a property that is induced by the spin-orbit interaction. In fact, according to the sum rule for XMLD the ratio of the integrated  $L_3$  to  $L_2$  intensities can be related to the anisotropic part of the  $3d$  spin-orbit interaction, which in turn is related to the MAE [9]. While the change in the integrated intensity is usually small (in the case of a half-filled shell essentially zero), the changes in the spectral structure of the AXMLD are very large for  $3d$  transition metal oxides. This is due to the fact that XA spectra are determined by electric-dipole selection rules restricting the set of final states reachable from the ground state and resulting in different transition probabilities from the exchange split core levels to the crystal field split empty  $d$  states.

In rare earth systems, AXMLD has recently been reported for Eu  $M_{4,5}$  in EuO [10]. It is interesting to compare these observations with those of  $3d$  metals, where the spin-orbit interaction is much smaller than the CEF interaction. For the atomic Fe, Co, and Ni  $3d$  shell the spin-orbit interaction is about 0.05, 0.07, and 0.08 eV, respectively, [11] and for Eu  $4f$  it is 0.16 eV [12]. While in rare earths the spin-orbit interaction is not reduced, in

$3d$  metals it is “quenched” (typically to  $\sim 10\%$  of its atomic value) due to the strong CEF interaction (1-2 eV). On the other hand, the electrostatic interactions, given by the Slater integrals, are comparable for both systems, e.g.,  $F^2 \approx 10$  eV [12].

By comparing  $4f$  with  $3d$  systems, we can investigate (i) the impact of a much reduced crystal field, (ii) whether for  $f$ -electron systems two fundamental spectra are needed and/or sufficient, and (iii) to what extent the  $4f$  orbitals are able to follow the rotation of the magnetization or that they are held back by the CEF and hybridization which couple the orbitals to the lattice.

Taking the spin-orbit interaction as a small perturbation on the CEF, as in the case of  $3d$  systems, the electron orbitals are firmly coupled to the lattice by CEF and hybridization. The associated orbital magnetic moment, and via spin-orbit coupling the spin magnetic moment, are oriented along the easy magnetization direction. An applied magnetic field rotates the spin, but the charge density remains fixed to the lattice. The change in the orbital magnetic moment value along different magnetization directions results in a weak magnetic anisotropy. In  $4f$  systems, by contrast, the spin-orbit coupling is strong and the CEF is weak, so that the charge density rotates with the total angular momentum which is aligned along the magnetization direction. The difference in energy associated with different orientations of the charge density results in a large magnetic anisotropy.

In this study we used EuO, a ferromagnetic semiconductor with a Curie temperature of 69 K that crystallizes in rocksalt structure. The motivation to study specifically EuO stems from its fascinating properties and technologically important features for spintronics research [13, 14]. 500 nm thick single crystalline EuO films were grown by reactive molecular-beam epitaxy [14]. The EuO was formed by evaporating pure Eu in a background pressure of  $3 \times 10^{-9}$  Torr  $O_2$  on a 1.3 nm SrO buffer layer deposited on top of a clean Si(001) surface and capped in situ with 10 nm amorphous Si to prevent oxidation during sample transfer [14]. The sample exhibited a Curie temperature of 69 K identical to the bulk value [15] and no significant in-plane magnetic anisotropy was observed. XA spectra were measured on beamline 4.0.2 at the Advanced Light Source providing  $(99 \pm 1)\%$  linearly polarized x rays. The x-ray polarization was oriented at an angle  $\phi$  to the EuO [100] axis. XMLD spectra were obtained in normal incidence at  $T=15$  K in total electron yield mode. External fields of 0.1 T provided by an eight-pole resistive electromagnet [16] are sufficient to align the Eu moments along any in plane direction. XMLD spectra,  $I_{\text{XMLD}}(\phi)$ , are obtained as the

difference between XA spectra with  $\mathbf{H}$  parallel and perpendicular to  $\mathbf{E}$ , i.e., at angles  $\phi$  and  $\phi + 90^\circ$  to the [100] axis. Since our experimental geometry is invariant for a reflection of both  $\mathbf{H}$  and  $\mathbf{E}$  with respect to  $\phi = 45^\circ$ , we find  $I_{\text{XMLD}}(90^\circ - \phi) = I_{\text{XMLD}}(\phi)$ . Therefore, we only have to consider  $0^\circ \leq \phi \leq 45^\circ$  in the following.

Figure 1(a) shows the Eu  $M_{4,5}$  XA spectrum measured in normal incidence at  $T = 15$  K with linearly polarized x rays. The spectral shape agrees well with previously reported Eu  $M_{4,5}$  XA spectra of  $\text{Eu}^{2+}$  [12]. A small additional intensity around 1133 eV is due to a 7.5%  $\text{Eu}_2\text{O}_3$  contribution in the near surface region probed by electron yield [17]. However, the  $\text{Eu}^{3+}$  ion with ground state  ${}^7F_0$  is expected to be non-magnetic [18]. Figure 1(b) shows the Eu  $M_{4,5}$  x-ray magnetic circular dichroism (XMCD), in agreement with earlier reports [19]. Figure 1(c) shows a set of XMLD spectra for  $0^\circ \leq \phi \leq 90^\circ$ . The magnitude of the signal spans the range of approximately  $\pm 15\%$  near the  $M_5$  edges. This is substantially larger than the XMLD signals observed at the transition metal  $L_3$  edges, which are typically  $\sim 5\%$  of the  $L_3$  intensity. Although, the angular dependence of the XMLD is very weak, a small variation of the XMLD signal, e.g., near 1156 eV, can be observed.

According to the description of the AXMLD in cubic  $3d$  metal systems [6], the angular dependent XMLD in the (001) plane is a linear combination of the two fundamental spectra,  $I_0$  and  $I_{45}$ , which are the XMLD spectra obtained for  $\phi = 0^\circ$  and  $45^\circ$ ,

$$I_{\text{XMLD}}(\phi) = \frac{1}{2} [I_0 + I_{45} + (I_0 - I_{45}) \cos 4\phi]. \quad (1)$$

Hence, the AXMLD contains a constant term, i.e., the averaged spectrum  $\frac{1}{2}(I_0 + I_{45})$ , and an angular dependent term,  $I_0 - I_{45}$ , varying as  $\frac{1}{2} \cos 4\phi$ . Since the variations in the XMLD are very small (only about 1% of the Eu  $M_5$  XA), these two linear combinations of  $I_0$  and  $I_{45}$  provide a better way of analyzing the angular dependence [10]. They have been extracted from Fig. 1(b) and are shown in Fig. 2(c).

If the CEF becomes zero, the  $4f$  sublevels are degenerate, making the  $4f$  state rotationally invariant, so that the  $3d \rightarrow 4f$  XMLD is the same at every angle, in which case  $I_0 = I_{45}$ . In rare earths, the CEF is very small, so that  $I_0 + I_{45} \gg I_0 - I_{45}$ . In contrast,  $3d$  systems with strong CEF interaction can quite often have  $I_0 + I_{45} \approx 0$  [7, 8]. This necessitates an interesting change in the spectral shape when going from weak to strong CEF interaction, since one would unlikely encounter that the XMLD signal disappears for intermediate CEF.

For further confirmation the measured spectra can be compared with multiplet calcula-

tions for  $\text{Eu}^{2+} 4f^7 \rightarrow 3d^9 4f^8$ , with parameters given in Ref. 12. This gives a good agreement with experimental results, as seen in Fig. 2. For Eu  $M_{4,5}$  the XA, XMCD, and averaged XMLD resemble the atomic case, however  $I_0 - I_{45}$  depends on the CEF. Interestingly, for a small CEF the shape of  $I_0 - I_{45}$  does not change, while the magnitude scales linearly with the CEF strength, or more specifically with the parameter  $V_0^4$  [10]. A quantitative good agreement is obtained for  $V_0^4 = 175$  meV, which is smaller than the  $4f$  spin-orbit splitting of 0.65 eV and the  $4f$  Coulomb interactions [12], both conserving spherical symmetry. The half-filled shell is actually an interesting case. The CEF for the half-filled shell  $f^7$  appears to be much larger than for other  $f^n$  configurations [20, 21]. While the reason for this remains largely unclear, it would support the large CEF found for EuO.

The calculations furthermore show that  $I_0 - I_{45}$  neither depends on the magnitude of the applied exchange field nor on the size of the  $4f$  spin-orbit interaction, while scaling the Slater integrals only gives a modest change in the shape and magnitude of  $I_0 - I_{45}$ . The symmetry, on the other hand, is of major importance and going from octahedral to tetrahedral environment the  $I_0 - I_{45}$  spectrum changes sign while roughly maintaining the same shape.

To summarize, the AXMLD at the  $\text{Eu}^{2+} M_{4,5}$  edges of EuO(001) is very well described with the model developed for cubic transition metal oxides [6–8]. Multiplet calculations show that the size of the anisotropic XMLD for Eu  $f^7$  is directly proportional to the effective CEF parameter  $V_0^4$ . The experimental spectra indicate a significant energy splitting of the  $4f$  orbitals. The resulting charge asphericity in each of the non-degenerate  $4f$  states means that pinning of the  $f$  states by the local environment becomes feasible and can be tuned by external conditions, chemical doping, and strain for use in device applications.

The Advanced Light Source is supported by the Director, Office of Science, Office of Basic Energy Sciences, of the U.S. Department of Energy under Contract No. DE-AC02-05CH11231.

- 
- [1] J. Petzold, J. Magn. Magn. Mater. **242-245**, 84 (2002).
  - [2] G. C. Hadjipanayis, J. Magn. Magn. Mater. **200**, 373 (1999).
  - [3] J. Coey, J. Magn. Magn. Mater. **248**, 441 (2002).
  - [4] K. O’Grady and H. Laidler, J. Magn. Magn. Mater. **200**, 616 (1999).

- [5] R. Wu and A. Freeman, *J. Magn. Magn. Mater.* **200**, 498 (1999).
- [6] E. Arenholz, G. van der Laan, R. V. Chopdekar, and Y. Suzuki, *Phys. Rev. B* **74**, 94407 (2006).
- [7] E. Arenholz, G. van der Laan, R. V. Chopdekar, and Y. Suzuki, *Phys. Rev. Lett.* **98**, 197201 (2007).
- [8] G. van der Laan, E. Arenholz, R. V. Chopdekar, and Y. Suzuki, *Phys. Rev. B* **77**, 064407 (2008).
- [9] G. van der Laan, *Phys. Rev. Lett.* **82**, 640 (1999).
- [10] G. van der Laan, E. Arenholz, A. Schmehl, and D. G. Schlom, *Phys. Rev. Lett.* **100**, 067403 (2008).
- [11] G. van der Laan and I. W. Kirkman, *J. Phys.: Condens. Matter* **4**, 4189 (1992).
- [12] B. T. Thole, G. van der Laan, J. C. Fuggle, G. A. Sawatzky, R. Karnatak, and J.-M. Esteve, *Phys. Rev. B* **32**, 5107 (1985).
- [13] A. Mauger and C. Godart, *Phys. Rep.* **141**, 51 (1986).
- [14] A. Schmehl, V. Vaithyanathan, A. Herrnberger, S. Thiel, C. Richter, M. Liberati, M. T. Heeg, L. Fitting-Kourkoutis, S. Mühlbauer, P. Böni, et al., *Nature Mater.* **6**, 882 (2007).
- [15] B. T. Matthias R. M. Bozorth and J. H. Van Vleck, *Phys. Rev. Lett.* **7**, 160 (1961).
- [16] E. Arenholz and S. O. Prestemon, *Rev. Sci. Instrum.* **76**, 083908 (2005).
- [17] E. Negusse, J. Holroyd, M. Liberati, J. Dvorak, Y. U. Idzerda, T. S. Santos, J. S. Moodera, and E. Arenholz, *J. Appl. Phys.* **99**, 08E507 (2006).
- [18] S. Kern and R. Kostelecky, *J. Appl. Phys.* **42**, 1773 (1971).
- [19] J. B. Goedkoop, B. T. Thole, G. van der Laan, G. A. Sawatzky, F. M. F. de Groot, and J. C. Fuggle, *Phys. Rev. B* **37**, 2086 (1988).
- [20] B. G. Wybourne, *Phys. Rev.* **148**, 317 (1966).
- [21] B. R. Judd, *Phys. Rev.* **162**, 28 (1967).

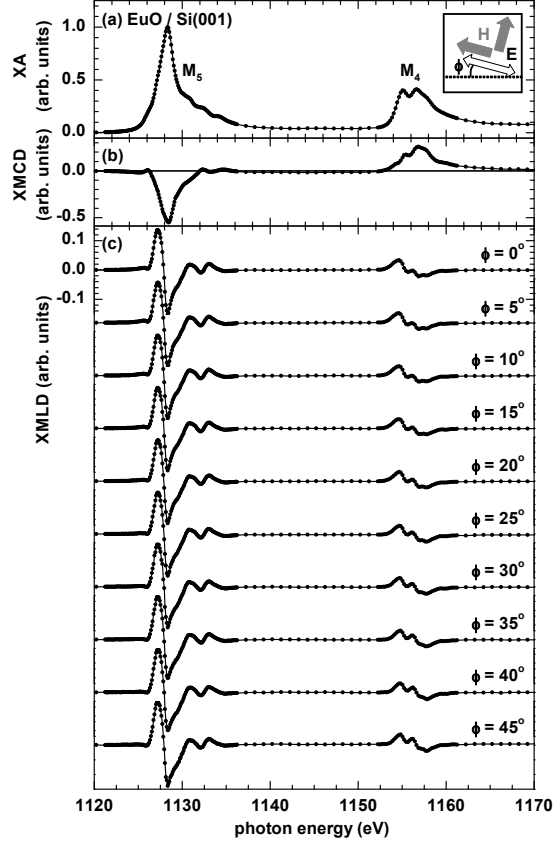


FIG. 1: Observed angular dependence of the Eu  $M_{4,5}$  XMLD in EuO/Si(001). (a) XA spectrum. (b) XMCD spectrum. (c) XMLD spectra showing small changes for  $0^\circ \leq \phi \leq 45^\circ$ . The inset in (a) depicts the experimental geometry indicating the linear polarization  $\mathbf{E}$  (white arrow) lies at an angle  $\phi$  to the [100] axis (dashed line) and applied external fields  $\mathbf{H}$  (gray arrows) at angles  $\phi$  and  $\phi + 90^\circ$ , respectively.



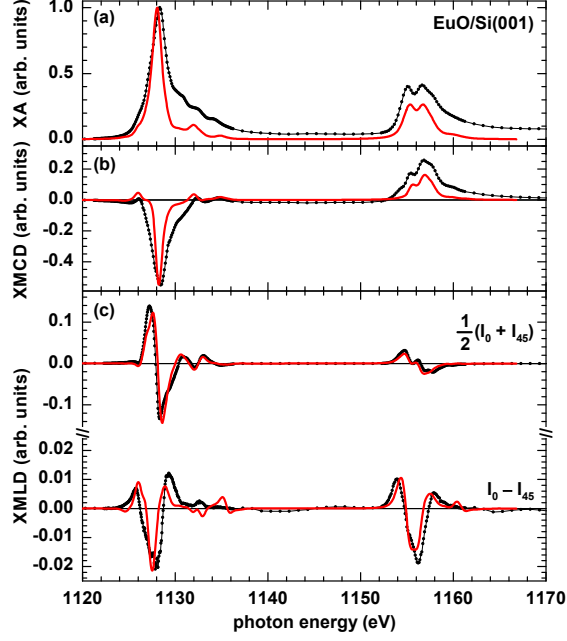


FIG. 2: (Color online) Comparison of experimental (black dots) and calculated (red lines) Eu  $M_{4,5}$  spectra. (a) XA spectrum. (b) XMCD spectrum. (c) Averaged XMLD,  $\frac{1}{2}(I_0 + I_{45})$  and difference spectrum,  $I_0 - I_{45}$ . The calculated spectra were broadened by an intrinsic lifetime using a Lorentzian of  $\Gamma = 0.25$  (0.5) eV for the  $M_5$  ( $M_4$ ) edge and an instrumental linewidth using a Gaussian of  $\sigma = 0.25$  eV.